JOURNAL OF SYNCHROTRON RADIATION
ISSN 1600-5775

Phosphorus *K*-edge XANES spectroscopy has probably often underestimated iron oxyhydroxide-bound P in soils

Jörg Prietzel[a]* and Wantana Klysubun[b]

[a]Lehrstuhl für Bodenkunde, Technische Universität München, Emil-Ramann-Straße 2, D-85354 Freising, Germany, and [b]Synchrotron Light Research Institute, 111 University Avenue, Nakhon Ratchasima 30000, Muang District, Thailand. *Correspondence e-mail: prietzel@wzw.tum.de

Received 18 June 2018
Accepted 18 September 2018

Edited by S. M. Heald, Argonne National Laboratory, USA

Keywords: Fe-bound P; ferrihydrite; goethite; organic P; P retention; P speciation; soil; IHP; LCF; *K*-edge XANES spectra.

Phosphorus (P) *K*-edge X-ray absorption near-edge structure (XANES) spectra of orthophosphate (oPO_4) bound to soil Fe^{III} minerals (*e.g.* ferrihydrite, goethite) show a pre-edge signal at 2148–2152 eV. It is unknown whether organic P bound to Fe^{III} oxyhydroxides also show this feature. Otherwise, Fe-bound soil P may be underestimated by P *K*-edge XANES spectroscopy, because a large portion of Fe oxyhydroxide-bound P in soils is organic P. *K*-edge XANES spectra were obtained for different organic P compounds present in soils [inositol hexaphosphate (IHP), glucose-6-phosphate (G6P), adenosine triphosphate (ATP)] after sorption to ferrihydrite or goethite and compared with spectra of oPO_4 adsorbed to these minerals. P sorption to ferrihydrite increased in the sequence IHP $\ll$ G6P < oPO_4 < ATP. P sorption to goethite increased in the sequence G6P < oPO_4 $\ll$ ATP = IHP. Pre-edge signals in P *K*-edge XANES spectra of organic P adsorbed to Fe oxyhydroxides were markedly smaller compared with those of oPO_4 adsorbed to these minerals and absent for Fe^{III} oxyhydroxide-bound ATP as well as goethite-bound IHP. Linear combination fitting (LCF) performed on spectra of IHP, G6P or ATP adsorbed to ferrihydrite or goethite, using only spectra of Fe^{III} oxyhydroxide-bound oPO_4 as reference compounds for Fe-bound P, erroneously assigned >93% (ferrihydrite) or >41% (goethite) of Fe-bound P to non-Fe-bound P species. Inclusion of Fe^{III} oxyhydroxide-bound IHP as reference compounds markedly increased the recovery of oxyhydroxide-bound organic P. Thus, Fe-bound soil P has probably often been underestimated by LCF in soil XANES studies where IHP adsorbed to ferrihydrite and to goethite were not included as reference compounds.

1. Introduction

Phosphorus (P) is an essential nutrient element for life and the P supply of terrestrial ecosystems is strongly dependent on the availability of soil P (Elser *et al.*, 2007; Achat *et al.*, 2016). Phosphorus in soils exists in various organic and inorganic forms with different availability to plants and microorganisms. Thus, different biotic P mobilization strategies are in effect for organic and inorganic P, and also the mobilization of P bound to Ca, Fe and Al soil minerals is executed through different processes (*e.g.* acidification, reduction, specific complexation of Ca, Al or Fe). Therefore, in addition to the quantification of the total soil P content, a correct discrimination and quantification of different soil P species is crucial for an assessment of the availability, turnover and long-term fate of soil P.

Traditionally, soil P is distinguished by wet-chemical methods into different P forms. Saunders & Williams (1955) developed a method to quantify organic *versus* inorganic P in

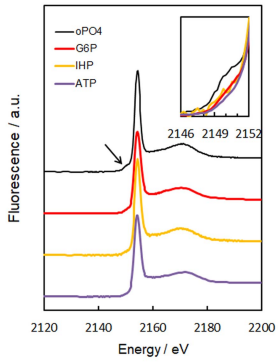

soils, which has been modified and optimized repeatedly (Walker & Adams, 1958; Talkner *et al.*, 2009). Organic and inorganic P adsorbed to short-range-order (SRO) and crystalline (CRY) pedogenic Fe, Al and Mn oxyhydroxides can be estimated, even though not quantified exactly (Prietzel, 2017), by extraction with acidic oxalate (SRO) or dithionite-citrate-bicarbonate solution (SRO+CRY) and subsequent P determination of the mobilized total P by ICP-OES and of mobilized orthophosphate (oPO_4) by colorimetry (*e.g.* Prietzel, Klysubun *et al.*, 2016; Werner *et al.*, 2017). Several protocols have been developed to quantify plant-available P in soils (*e.g.* Bray & Kurtz, 1945; Olsen *et al.*, 1954; Mehlich, 1984). A widely used wet-chemical method (*cf.* Cross & Schlesinger, 1995) for partitioning soil P into several pools with different plant availability has been developed by Hedley *et al.* (1982). Often, the Hedley P fractions, even though operationally defined (Zederer & Talkner, 2018), have been assigned to different soil P forms. The NaOH-soluble P fraction in the sample residue after $NaHCO_3$ extraction was proposed to consist of P bound to pedogenic Fe^{III} or Al minerals, and the HCl-soluble P fraction in the residue after NaOH extraction was proposed to be Ca-bound P, as, for example, apatite (Tiessen *et al.*, 1984). However, recent studies (*e.g.* Hunger *et al.*, 2005) showed that this assignment is not entirely correct. Moreover, neither Hedley fractionation nor any other fractionation protocol can distinguish exactly between Fe-bound P and Al-bound P. However, such a discrimination would be desirable, since P bound to pedogenic Al minerals is more susceptible to mobilization during progressive soil acidification than P bound to pedogenic Fe^{III} minerals because of the considerably larger solubility of Al compared with Fe oxyhydroxides oxides under acidic conditions like pH ≤ 5. On the other hand, P bound to Fe^{III} soil minerals is more susceptible to mobilization by redox processes (*e.g.* Fe oxyhydroxide dissolution after soil water-logging or inundation).

Recently, synchrotron-based P *K*-edge X-ray absorption near-edge structure (XANES) spectroscopy has emerged as a powerful, non-invasive, direct technique for the P speciation in soils (for example, Beauchemin *et al.*, 2003; Kruse & Leinweber, 2008; Prietzel *et al.*, 2013; Prietzel, Klysubun *et al.*, 2016; Giguet-Covex *et al.*, 2013; Eriksson *et al.*, 2016). Using XANES spectroscopy, oPO_4 bound to different elements (*e.g.* Al, Fe, Ca) can be distinguished by specific spectra patterns. Thus, in contrast to Al- or Fe-bound P, oPO_4 bound to Ca has *K*-edge XANES spectra characterized by a tailing shoulder of its white-line and specific post-edge signals produced by P 1*s* to Ca(3*p*)–O(2*p*) electronic transitions dependent on the type of Ca-phosphate mineral. In contrast, oPO_4 bound to Fe^{III} minerals, such as ferrihydrite, goethite or hematite, is characterized by a pre-edge peak, which is not visible for Al-bound or Ca-bound oPO_4 (Hesterberg *et al.*, 1999; Khare *et al.*, 2004, 2005; Adam, 2017). This pre-edge peak is produced by P 1*s* to Fe(4*p*)–O(2*p*) electronic transitions and indicates the presence of P—O—Fe covalent bonds in Fe^{III} phosphate minerals such as strengite ($FePO_4{\cdot}2H_2O$). The fact that such pre-edge features are also present in P *K*-edge XANES spectra of oPO_4 adsorbed to pedogenic Fe^{III} oxyhydroxides proves specific oPO_4 sorption to these oxyhydroxides involving inner-sphere complexation and ligand exchange (Khare *et al.*, 2004, 2005).

Interestingly, a recent study on the P speciation of different forest soils using P *K*-edge XANES spectroscopy (Prietzel, Klysubun *et al.*, 2016) showed surprisingly small percentages of P bound to Fe^{III} compared with Al minerals, even for soils with large contents of pedogenic Fe^{III} minerals as well as P bound to these minerals. For several soils formed on calcareous parent material, which contained significant amounts of SRO as well as well crystallized Fe oxyhydroxides, no Fe-bound P was detected at all, even though oPO_4 added to mixtures of ferrihydrite and poorly crystalline calcite of similar particle size in a recent study by Adam (2017) showed marked pre-edge features, indicating oPO_4 sorption to ferrihydrite. This raises the question as to whether a significant part of the Fe-bound P present in soils does not show a distinct pre-edge feature and thus erroneously may be assigned to other P species than Fe-bound P during deconvolution of P *K*-edge XANES spectra. Here, we show that various organic P forms [inositol hexaphosphate (IHP), glucose-6-phosphate (G6P) and adenosine triphosphate (ATP)] retained by ferrihydrite show a less pronounced pre-edge feature than oPO_4 retained by ferrihydrite (IHP, G6P), or no pre-edge feature at all (ATP). Moreover, we show that, in contrast to oPO_4, the pre-edge peak in the XANES spectra of the investigated organic P forms adsorbed to goethite is either completely absent (IHP, ATP) or only small (G6P). Together with the facts that (i) a large portion of the P in soil solution is organic P (Qualls *et al.*, 1991; 2000; Kaiser *et al.*, 2000; 2003; Bol *et al.*, 2016), (ii) the retention of organic P by soils (Harrison, 1987; Berg & Joern, 2006; Zederer & Talkner, 2018) and pedogenic soil minerals (Celi *et al.*, 1999; Prietzel, Harrington *et al.*, 2016) often is as large as or even larger than the retention of oPO_4, and (iii) most organic P in mineral soils is probably bound to Al and particularly Fe oxyhydroxides (Talkner *et al.*, 2009; Vincent *et al.*, 2012; Grand & Lavkulich, 2015; Werner *et al.*, 2017; Zederer & Talkner, 2018), our finding suggests underestimation of Fe-bound soil P by *K*-edge XANES spectroscopy.

2. Material and methods

2.1. Sorption experiments

Six-line ferrihydrite [specific surface area (SSA) measured by BET: 218 $m^2\,g^{-1}$ at pH 3.0 and at pH 6.0] and goethite (SSA: 30 $m^2\,g^{-1}$ at pH 3.0 and 21 $m^2\,g^{-1}$ at pH 6.0) were synthesized according to Schwertmann & Cornell (1991). Subsamples of either 30 mg homogenized ferrihydrite (24 subsamples) or 30 mg goethite (24 subsamples) were filled into 100 ml polythene bottles. Then, we added 99 ml 0.1 *M* acetic acid/Na acetate buffer solution, with the pH adjusted to 3.0 or 6.0, each for 12 ferrihydrite and 12 goethite subsamples, and stirred the mixtures. After 20 minutes, three replicate

suspensions of each mineral-pH variant were treated with either (*a*) 1 ml 0.0323 *M* NaH_2PO_4 (m = 120 g mol^{-1}; Merck Comp.), (*b*) 1 ml 0.0323 *M* IHP [phytic acid Na salt ($C_6H_{18}O_{24}P_6$·Na); m = 660 g mol^{-1}; Sigma Aldrich], (*c*) 1 ml 0.0323 *M* adenosine-5′-trihydrogentriphosphate (ATP $C_{10}H_{16}N_5O_{13}P_3$; m = 507 g mol^{-1}; Sigma Aldrich) or (*d*) 1 ml 0.0323 *M* glucose-6-phosphate (G6P; m = 260 g mol^{-1}; Sigma Aldrich) to yield a final solution concentration of 10 mg L^{-1} P. Immediately after P addition, the suspensions were stirred again and allowed to settle for 18 h at 293 K in the dark. Then, the samples were membrane-filtered (cellulose nitrate; Sartorius; 0.45 µm pore size). In the filtrates, we analyzed solution P concentrations after retention equilibrium by ICP-OES (Varian Vista Pro). Then we calculated the P amount retained by the minerals for each experimental variant and replicated by subtracting the P concentration in the solution at the end of the experiment from the respective initial P concentration. Air-dried solid phase residues were scraped from the filters with a spatula and homogenized for XANES spectra acquisition. A similar set of mineral-pH variant suspensions was treated with 1 ml 0.00323 *M* oPO_4, IHP, G6P and ATP solution, resulting in initial P concentrations of 1 mg L^{-1}. As with the 10 mg L^{-1} P variant, the suspensions after P addition were stirred, membrane-filtrated after 18 settling, and P solution concentrations in the filtrates were analyzed by ICP-OES.

2.2. Phosphorus speciation by P *K*-edge XANES spectroscopy

For the different filter residues, we acquired P *K*-edge XANES spectra at beamline 8 of the Synchrotron Light Research Institute (SLRI) in Nakhon Ratchasima, Thailand (Klysubun *et al.*, 2012). Briefly, we spread sample powder as thin, homogeneous film on P-free Kapton tape (Lanmar Inc., Northbrook, IL, USA) and mounted the tape on a sample holder. Then we scanned the X-ray photon energy using an InSb(111) double-crystal monochromator with an energy resolution of $\Delta E/E = 3 \times 10^{-4}$). We recorded all spectra in fluorescence mode with a 13-element germanium detector. To increase fluorescence yield, we placed the sample holder at a 45° angle to the incident monochromatic beam (beam size 12 mm × 1 mm). We constantly purged the sample compartment with helium gas to minimize X-ray absorption by air surrounding the sample. For acquisition of P *K*-edge XANES spectra, we calibrated the monochromator with elemental P (E_0 = 2145.5 eV). This was repeated every 12 h, and there was no indication of E_0 movement during the entire beam time. After calibration, we acquired spectra in the energy range from 2045.5 eV to 2345.5 eV with a 2 s dwell time per energy step. Energy steps were as follows: from 2045.5 to 2125.5 eV and from 2195.5 to 2345.5 eV: energy step of 5 eV; from 2125.5 to 2135.5 eV and from 2165.5 to 2195.5 eV: energy step of 1 eV; and finally from 2135.5 to 2165.5 eV: energy step of 0.25 eV. For each sample, we acquired two spectra. Multiple spectra acquired for each sample were always identical, which rules out artificial sample changes caused by radiation damage. Replicate spectra obtained for a given sample were merged using the software *ATHENA* (Ravel & Newville, 2005). All merged spectra then were subject to edge-step normalization and linear combination fitting (LCF) in the energy range 2140–2190 eV using the protocol of Werner & Prietzel (2015). In a first run, we used only Fe^{III} phytate, oPO_4 adsorbed to ferrihydrite or goethite, respectively, and amorphous $FePO_4$ as reference compounds for Fe-bound P. Additionally, we included spectra of oPO_4 adsorbed to boehmite and of amorphous $AlPO_4$ as proxies for Al-bound P, of apatite as proxy for Ca-bound P, and of Na-IHP as proxy for free organic P in the LCF reference compound set in order to check the LCF results for erroneous P form assignments. The spectra of all standards have been shown and described in detail by Prietzel, Harrington *et al.* (2016). In a second run, we additionally included reference spectra of IHP adsorbed to ferrihydrite or goethite, respectively.

3. Results

3.1. Retention of different P compounds by ferrihydrite and goethite

The extent of P retention by ferrihydrite and goethite differed among the P compounds and also depended on initial solution P concentration, mineral type and pH (Table 1). For both minerals, P retention was always larger at pH 3 than at pH 6. For the experimental variants with low P loading (initial P solution concentration: 1 mg L^{-1}), P retention by ferrihydrite increased in the order: IHP ≪ G6P ≤ oPO_4 < ATP (Table 1; Fig. 1), resulting in P equilibrium solution concentrations between 0.01 and 0.79 mg L^{-1}. The percentage of retained P applied as IHP was 21% (pH 3) and 30% (pH 6), whereas almost all P (>97%) applied as oPO_4, G6P or ATP was retained by ferrihydrite at pH 3 and 83–97% of the P applied as oPO_4, G6P or ATP was retained by ferrihydrite at pH 6. P retention by goethite increased in the order: G6P = oPO_4 (40–49% P retention; equilibrium solution P concentration 0.5–0.6 mg L^{-1}) ≪ IHP = ATP (78–94% P retention; 0.06–0.18 mg L^{-1} P). On a mineral mass basis (Fig. 1; left panels), retention of oPO_4 and G6P was larger for ferrihydrite than for goethite, ATP retention was similar for both minerals, and IHP retention was markedly larger for goethite than for ferrihydrite. SSA-normalized P retention (Fig. 1; right panels) was always larger for goethite than for ferrihydrite. In the variants with high P loading (initial P concentration: 10 mg L^{-1}), P retention by ferrihydrite increased in the order: IHP ≪ G6P < oPO_4 < ATP (Table 1; Fig. 2). For all P compounds except IHP, P retention decreased strongly with increasing pH. P retention by goethite increased in the order: G6P ≤ oPO_4 (3–5% P retention; equilibrium solution P concentration 9.5–9.7 mg L^{-1}) ≪ IHP = ATP (9–11% P retention; 8.9–9.1 mg L^{-1} P). On a mineral mass basis (Fig. 2, left panels), ferrihydrite was considerably more efficient than goethite in retaining all P compounds except IHP. In contrast, on a surface area basis (Fig. 2, right panels), most often goethite was a more effective P sorbent than ferrihydrite.

Table 1
Equilibrium solution P concentration and percentage of initial solution P retained by ferrihydrite and goethite for different P compounds [orthophosphate (oPO_4), inositol hexaphosphate (IHP), glucose-6-phosphate (G6P), adenosine triphosphate (ATP)], initial solution P concentrations (1 and 10 mg L^{-1}) and equilibrium pH values (3.0, 6.0).

			Initial solution P concentration 1 mg L^{-1}		Initial solution P concentration 10 mg L^{-1}	
			Equilibrium solution P concentration (mg L^{-1} P)	Percentage of applied P retained	Equilibrium solution P concentration (mg L^{-1} P)	Percentage of applied P retained
Ferrihydrite	pH 3	oPO_4	0.02 ± 0.06	98	4.9 ± 0.1	51
		IHP	0.79 ± 0.01	21	9.8 ± 0.1	2
		G6P	0.02 ± 0.00	98	7.3 ± 0.3	27
		ATP	0.01 ± 0.01	99	3.7 ± 0.1	63
	pH 6	oPO_4	0.17 ± 0.05	83	7.2 ± 0.1	28
		IHP	0.70 ± 0.08	30	9.9 ± 0.2	1
		G6P	0.17 ± 0.04	83	8.1 ± 0.0	19
		ATP	0.03 ± 0.00	97	7.1 ± 0.2	29
Goethite	pH 3	oPO_4	0.52 ± 0.05	48	9.5 ± 0.2	5
		IHP	0.10 ± 0.01	90	8.9 ± 0.1	11
		G6P	0.51 ± 0.02	49	9.5 ± 0.0	5
		ATP	0.06 ± 0.02	94	8.9 ± 0.1	11
	pH 6	oPO_4	0.56 ± 0.01	44	9.6 ± 0.2	4
		IHP	0.12 ± 0.01	88	9.1 ± 0.1	9
		G6P	0.60 ± 0.00	40	9.7 ± 0.1	3
		ATP	0.18 ± 0.02	78	9.1 ± 0.1	9

3.2. P *K*-edge XANES spectra of different P compounds adsorbed to ferrihydrite and goethite

The P *K*-edge XANES spectrum oPO_4 adsorbed to ferrihydrite at solution pH 3 (Fig. 3*a*) shows a distinct pre-edge feature in the energy range 2148–2151 eV (see arrow). Closer inspection (inserted panel) reveals a small pre-edge signal also for G6P and IHP, which is absent for ATP. At solution pH 6 (Fig. 3*b*), the pre-edge signal of oPO_4 adsorbed to ferrihydrite is much smaller than that observed at pH 3, and no signals are visible for the organic P compounds. The P *K*-edge XANES spectra of oPO_4 adsorbed to goethite also show a pre-edge feature at solution pH 3 (Fig. 3*c*) and pH 6 (Fig. 3*d*). However, the pre-edge signal of oPO_4 adsorbed to goethite at pH 3 is

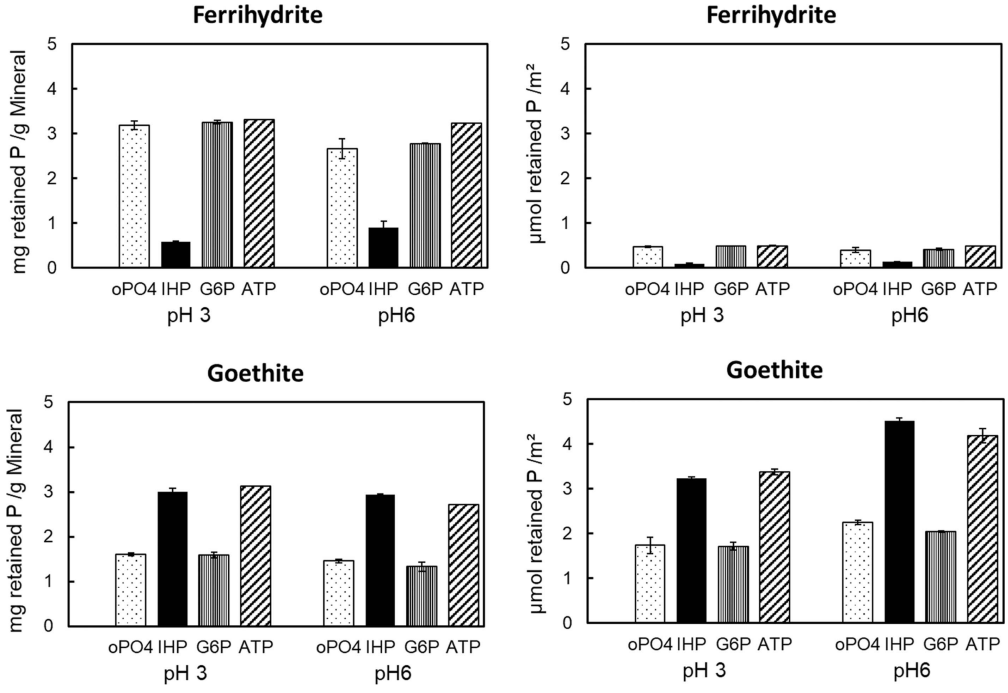

Figure 1
Retention of P applied as orthophosphate (oPO_4), inositol hexaphosphate (IHP), glucose-6-phosphate (G6P) and adenosine triphosphate (ATP; initial P concentration in all sorbents 1 mg L^{-1}) by ferrihydrite (upper panels) and goethite (lower panels).

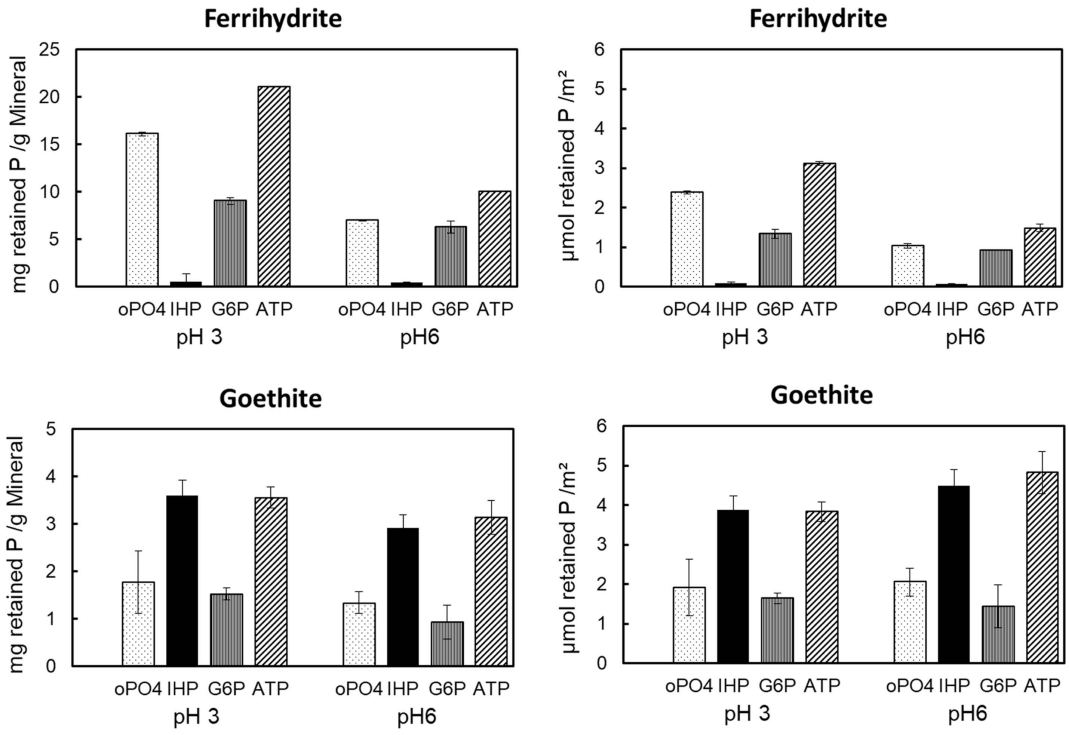

Figure 2
Retention of P applied as orthophosphate (oPO_4), inositol hexaphosphate (IHP), glucose-6-phosphate (G6P) and adenosine triphosphate (ATP; initial P concentration in all sorbents 10 mg L^{-1}) by ferrihydrite (upper panels) and goethite (lower panels).

Table 2
Overview of pre-edge signal intensity for P *K*-edge XANES spectra of orthophosphate and different organic P compounds adsorbed to ferrihydrite and goethite at pH 3.0 and pH 6.0.

++: large; +: moderate; (+): small; –: absent.

	Ferrihydrite		Goethite	
	pH 3.0	pH 6.0	pH 3.0	pH 6.0
Orthophosphate	++	+	+	+
Inositol hexaphosphate	(+)	–	–	–
Glucose-6-phosphate	(+)	–	(+)	(+)
Adenosine triphosphate	–	–	–	–

smaller than that of oPO_4 adsorbed to ferrihydrite at pH 3. In contrast to ferrihydrite, no pre-edge signals are visible for IHP or ATP adsorbed to goethite at pH 3 and 6, whereas G6P adsorbed to goethite shows a pre-edge-signal at both pH values, which was not present for G6P adsorbed to ferrihydrite. In summary (Table 2), (i) the pre-edge peaks of organic P compounds adsorbed to ferrihydrite or goethite are much smaller than that of oPO_4 adsorbed to the same mineral and often completely absent (ATP; IHP adsorbed to goethite). Moreover, (ii) a pH effect on pre-edge signal intensity was observed for ferrihydrite, but not for goethite.

3.3. P species as quantified by deconvolution of the P *K*-edge XANES spectra

3.3.1. Experimental variants with different P compounds adsorbed to ferrihydrite. LCF of the P *K*-edge XANES spectra acquired for IHP, ATP or G6P adsorbed to ferrihydrite, using only the spectra of (1) oPO_4 adsorbed to ferrihydrite, (2) amorphous $FePO_4$ and (3) Fe^{III} phytate, but not that of IHP adsorbed to ferrihydrite as reference compounds for Fe-bound P, in addition to the spectra of (4) oPO_4 adsorbed to boehmite and (5) amorphous $AlPO_4$ (proxies for Al-bound P), (6) apatite (proxy for Ca-bound P) and (7) Na phytate (proxy for free organic P) erroneously assigned almost all (>94%) of organic P bound to ferrihydrite to other P forms than Fe-bound P, mostly to oPO_4 adsorbed to boehmite and to free organic P (Table 3). Inclusion of IHP adsorbed to ferrihydrite as reference compound markedly improved the fit quality as indicated by decreased *R* factors. Moreover, the percentage of Fe-bound P erroneously assigned to other P forms (mostly free organic P) decreased to 0–56%, depending on the organic P species adsorbed to ferrihydrite.

3.3.2. Experimental variants with different P compounds adsorbed to goethite. LCF of the P *K*-edge XANES spectra acquired for IHP, ATP or G6P adsorbed to goethite, using only the spectra of (1) oPO_4 adsorbed to goethite, (2) amorphous $FePO_4$ and (3) Fe^{III} phytate, but not that of IHP adsorbed to goethite as reference compounds for Fe-bound P, in addition to the spectra (4)–(7) described in Section 3.3.1 erroneously assigned 42–82% of the organic P bound to goethite to other P forms than Fe-bound P, mostly to free organic P (Table 4). Inclusion of IHP adsorbed to goethite as reference compound markedly improved the fit quality as indicated by decreased *R* factors. Moreover, the percentage of Fe-bound P erroneously assigned to other P forms (mostly free organic P) decreased to 0–32%, depending on the organic P species adsorbed to goethite.

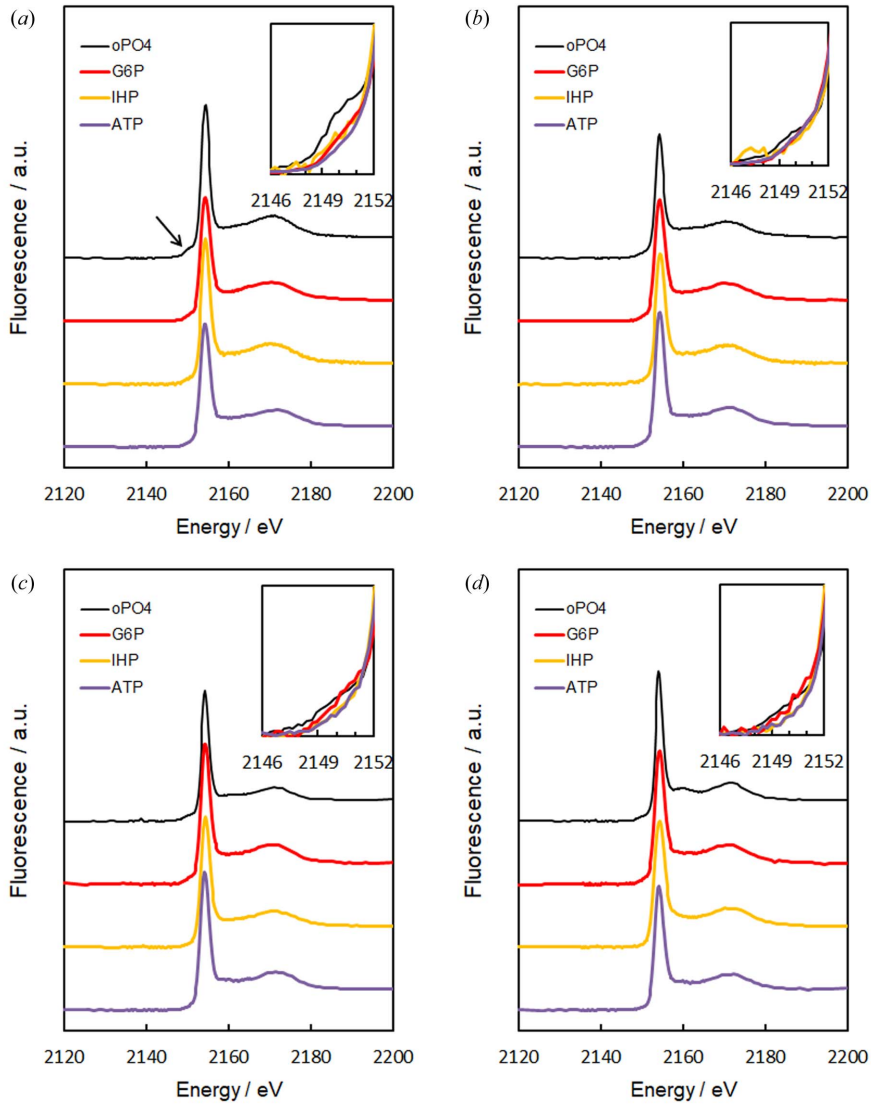

Figure 3
Edge-normalized P *K*-edge XANES spectra of different P forms retained by ferrihydrite (*a*, *b*) and goethite (*c*, *d*) at solution pH values of 3.0 (left panels) and 6.0 (right panels). Small inserted panels show the energy region 2146–2152 eV.

4. Discussion

In our study, as observed in earlier P-XANES studies by Hesterberg *et al.* (1999) and Khare *et al.* (2004, 2005), oPO_4 retained by either ferrihydrite or goethite showed a marked pre-edge signal. This is in line with the well known fact that inner-sphere complexation and surface precipitation are dominant oPO_4 retention mechanisms of these minerals (*e.g.* Tejedor-Tejedor & Anderson, 1986; Persson *et al.*, 1996; Hiemstra & van Riemsdijk, 1996). The results of our comparison of mass and surface-area-based retention efficiencies are in line with earlier reports. The superior oPO_4 retention efficiency of ferrihydrite compared with goethite is primarily due to its larger SSA, even though the stronger pre-edge feature of oPO_4 retained by ferrihydrite compared with oPO_4 retained by goethite, also reported by Hesterberg *et al.* (1999), indicates a greater relevance of ligand exchange for oPO_4 binding by ferrihydrite compared with goethite. The fact that IHP only shows a small pre-edge feature when retained by ferrihydrite at pH 3, and no pre-edge feature when retained by ferrihydrite at pH 6 or when retained by goethite at any pH (Table 2), suggests that inner-sphere complexation of IHP-P plays only a minor role for IHP retention by both minerals. Our observation supports earlier results of Johnson *et al.* (2012), but is in contradiction to statements of Ognalaga *et al.* (1994) and Celi *et al.* (1999). According to Johnson *et al.* (2012), hydrogen bonding between IHP P–O groups and H_2O molecules adsorbed to the goethite surface are responsible for the effective IHP retention by goethite also at high pH values. Inner-sphere complexation and surface precipitation were disproved by Fourier transform infrared spectroscopy in the study of Johnson *et al.* (2012). In contrast to goethite, about 40% of the pore volume of ferrihydrite is present as micropores <0.2 nm (Goebel *et al.*, 2017). These micropores are too small to become entered by the large, spherical IHP molecules (Shang *et al.*, 1992). Hence, the portion of total SSA which is not provided by micropores and thus is accessible to IHP is smaller for ferrihydrite than for goethite on a mineral mass basis. This fact explains the more efficient IHP sorption by goethite compared with ferrihydrite (Figs. 1 and 2).

The ATP molecule (m = 507 g mol^{-1}) is considerably smaller than the IHP molecule (m = 660 g mol^{-1}). Moreover, it has a rod-like instead of a spherical shape, with the two of the three phosphate groups located at the rod terminus (Berg & Joern, 2006). In contrast to IHP and similar to oPO_4, the terminal phosphate group of ATP can enter at least some ferrihydrite micropores and thus can utilize a larger portion of the ferrihydrite SSA. This circumstance explains the more efficient retention of ATP compared with IHP by ferrihydrite. As reported earlier (Shang *et al.*, 1992), also in our study G6P was retained more efficiently than IHP by ferrihydrite, while the opposite was the case for goethite (Table 1; Figs. 1, 2). The more effective retention of G6P by ferrihydrite compared with IHP can be explained by the smaller molecule size of G6P compared with IHP, allowing increased access to micropores in the ferrihydrite surface. The presence of an, albeit small, pre-edge signal in the P *K*-edge XANES spectra of G6P adsorbed to either ferrihydrite or goethite (Table 2) contrasts to the absence of such features for adsorbed ATP. It suggests that inner-sphere complexation

Table 3
Assignment of inositol hexaphosphate (IHP), glucose-6-phosphate (G6P) and adenosine triphosphate (ATP) (initial P concentration in all sorbents 10 mg L^{-1}) adsorbed to ferrihydrite to different P species by LCF performed on the respective P *K*-edge XANES spectra using the protocol of Werner & Prietzel (2015) and the reference compounds presented by Prietzel, Harrington *et al.* (2016).

		Percentage of total P assigned by LCF								
Sample		IHP adsorbed to ferrihydrite	oPO_4 adsorbed to ferrihydrite	Amorphous $FePO_4$	Fe^{III} phytate	oPO_4 adsorbed to boehmite	Amorphous $AlPO_4$	Free IHP	Apatite	*R* factor
Run 1: IHP adsorbed to ferrihydrite not included in standard set used for LCF										
IHP adsorbed	pH 3	—	0	0	0	30	0	70	0	0.00282
to ferrihydrite	pH 6	—	0	0	0	26	0	74	0	0.00256
G6P adsorbed	pH 3	—	0	6	0	5	0	89	0	0.00147
to ferrihydrite	pH 6	—	0	0	0	13	0	87	0	0.00289
ATP adsorbed	pH 3	—	0	0	0	8	0	92	0	0.00279
to ferrihydrite	pH 6	—	0	0	0	24	0	76	0	0.00200
Run 2: IHP adsorbed to ferrihydrite included in standard set										
IHP adsorbed	pH 3	100	0	0	0	0	0	0	0	0.00000
to ferrihydrite	pH 6	100	0	0	0	0	0	0	0	0.00000
G6P adsorbed	pH 3	37	7	0	0	0	0	56	0	0.00071
to ferrihydrite	pH 6	69	0	0	0	0	0	31	0	0.00159
ATP adsorbed	pH 3	55	0	0	0	8	0	45	0	0.00108
to ferrihydrite	pH 6	61	0	0	0	11	0	27	0	0.00084

Table 4
Assignment of inositol hexaphosphate (IHP), glucose-6-phosphate (G6P) and adenosine triphosphate (ATP) (initial P concentration in all sorbents 10 mg L^{-1}) adsorbed to goethite to different P species by LCF performed on the respective P *K*-edge XANES spectra using the protocol of Werner & Prietzel (2015) and the reference compounds presented by Prietzel, Harrington *et al.* (2016).

		Percentage of total P assigned by LCF								
Sample		IHP adsorbed to goethite	oPO_4 adsorbed to goethite	Amorphous $FePO_4$	Fe^{III} phytate	oPO_4 adsorbed to boehmite	Amorphous $AlPO_4$	Free IHP	Apatite	*R* factor
Run 1: IHP adsorbed to goethite not included in standard set used for LCF										
IHP adsorbed	pH 3	—	42	0	0	0	0	58	0	0.00446
to goethite	pH 6	—	20	0	0	0	0	80	0	0.00569
G6P adsorbed	pH 3	—	42	9	0	0	0	49	0	0.00054
to goethite	pH 6	—	18	0	0	0	0	82	0	0.00207
ATP adsorbed	pH 3	—	49	0	0	0	0	51	0	0.00098
to goethite	pH 6	—	58	0	0	0	0	37	5	0.00202
Run 2: IHP adsorbed to goethite included in standard set										
IHP adsorbed	pH 3	100	0	0	0	0	0	0	0	0.00000
to goethite	pH 6	100	0	0	0	0	0	0	0	0.00000
G6P adsorbed	pH 3	47	25	10	0	0	0	18	0	0.00023
to goethite	pH 6	56	26	0	0	0	0	18	0	0.00076
ATP adsorbed	pH 3	56	28	0	0	0	0	15	0	0.00060
to goethite	pH 6	44	24	0	0	19	0	13	0	0.00039

contributes to the retention of G6P-P, but not of ATP-P, by ferrihydrite and goethite.

Taking into account that (i) ferrihydrite and goethite are the most important P-retaining Fe oxyhydroxides in most soils; (ii) P in soil seepage water is mainly organic P and only to a small extent oPO_4 (Qualls *et al.*, 1991, 2000; Kaiser *et al.*, 2000, 2003; Bol *et al.*, 2016); (iii) the majority of the P bound in mineral soils (Harrison, 1987; Zederer & Talkner *et al.*, 2018), as well as the majority of P bound to pedogenic Al and Fe minerals (Prietzel, Harrington *et al.*, 2016; Werner *et al.*, 2017), is organic rather than inorganic P; and finally that (iv) IHP constitutes a large portion or even the majority of organic P in many soils (Harrison, 1987; Ognalaga *et al.*, 1994; Turner *et al.*, 2002), our results suggest that Fe-bound P is probably underestimated by LCF conducted on P *K*-edge XANES spectra, when spectra of IHP adsorbed to ferrihydrite and of IHP adsorbed to goethite are not included as reference compounds in addition to spectra of oPO_4 adsorbed to these minerals. The underestimation is caused by the fact that, in contrast to oPO_4 adsorbed to ferrihydrite or goethite, pre-edge signals in the P *K*-edge XANES spectra of many organic P compounds, including IHP, adsorbed to ferrihydrite or

goethite are most often only weak or completely absent. The underestimation probably contributes to the small percentages of Fe-bound P compared with Al-bound P reported for many acidic soils using P *K*-edge XANES spectroscopy (*e.g.* Giguet-Covex *et al.*, 2013; Eriksson *et al.*, 2016; Prietzel, Klysubun *et al.*, 2016) and probably also to the virtual absence of Fe-bound P in calcareous soils (Prietzel, Klysubun *et al.*, 2016). In our experimental variants with G6P and ATP as organic P compounds adsorbed to ferrihydrite or goethite, inclusion of IHP adsorbed to the respective mineral as reference compound in LCF markedly reduced but not completely removed the underestimation of Fe-bound P. Additional inclusion of G6P or ATP adsorbed to the respective mineral as LCF reference compounds would probably have removed the underestimation of these organic P compounds in our experiment. Unfortunately, such inclusion is not feasible for real soils, where, in addition to the reference compounds used in our experiment, several other candidate P forms have to be included in the reference set, because inclusion of too many reference compounds may produce erroneous LCF results because of model over-parameterization (Calvin, 2013) and thus should be avoided. However, the majority of organic P in most soils is IHP (Harrison, 1987; Ognalaga *et al.*, 1994; Turner *et al.*, 2002). Thus, inclusion of IHP adsorbed to ferrihydrite and of IHP adsorbed to goethite will probably in many cases suffice to marginalize any underestimation of Fe^{III}-bound P in soils by LCF conducted on P *K*-edge XANES spectra. Moreover, additional ^{31}P-NMR spectroscopy performed on NaOH-EDTA extracts of a soil sample of interest (*e.g.* Cade-Menun & Liu, 2013) can identify the most relevant organic P species in that sample. The P *K*-edge XANES spectra of this particular organic P compound adsorbed to ferrihydrite and/or goethite might be used as reference(s) in LCF performed on the P XANES spectrum of that sample. Furthermore, for some soils the presence of either ferrihydrite or goethite may be ruled out by results of mineralogical and/or wet-chemical analyses, and the spectra of organic P adsorbed to the respective Fe oxyhydroxide can be removed from the reference compound set used for LCF.

Acknowledgements

We gratefully acknowledge the assistance of Sigrid Hiesch, Monika Weber and Christine Pfab during conduction of the sorption experiments. We thank the staff of beamline 8 for their experimental support.

Funding information

This project was carried out in the framework of the Priority Programme 1685 'Ecosystem Nutrition: Forest Strategies for limited Phosphorus Resources' funded by the DFG (Grant Pr 534/6-2).

References

Achat, D. L., Pousse, N., Nicolas, M., Brédoire, F. & Augusto, L. (2016). *Biogeochemistry*, **127**, 255–272.
Adam, N. (2017). *Soil Sci. Soc. Am. J.* **81**, 1079–1087.
Beauchemin, S. D., Hesterberg, D., Chou, J., Beauchemin, M., Simard, R. R. & Sayers, D. E. (2003). *J. Environ. Qual.* **32**, 1809–1819.
Berg, A. S. & Joern, B. C. (2006). *J. Environ. Qual.* **35**, 1855–1862.
Bol, R., Julich, D., Brödlin, D., Siemens, J., Kaiser, K., Dippold, M. A., Spielvogel, S., Zilla, T., Mewes, D., von Blanckenburg, F., Puhlmann, H., Holzmann, S., Weiler, M., Amelung, W., Lang, F., Kuzyakov, Y., Feger, K., Gottselig, N., Klumpp, E., Missong, A., Winkelmann, C., Uhlig, D., Sohrt, J., von Wilpert, K., Wu, B. & Hagedorn, F. (2016). *J. Plant Nutr. Soil Sci.* **179**, 425–438.
Bray, R. H. & Kurtz, L. T. (1945). *Soil Sci.* **59**, 39–46.
Cade-Menun, B. & Liu, C. W. (2013). *Soil Sci. Soc. Am. J.* **78**, 19–37.
Calvin, S. (2013). *EXAFS for Everyone*, 1st ed., p. 457. London: CRC Press.
Celi, L., Lamacchia, S., Marsan, F. A. & Barberis, E. (1999). *Soil Sci.* **164**, 574–585.
Cross, A. F. & Schlesinger, W. H. (1995). *Geoderma*, **64**, 197–214.
Elser, J. J., Bracken, M. E. S., Cleland, E. E., Gruner, D. S., Harpole, W. S., Hillebrand, H., Ngai, J. T., Seabloom, E. W., Shurin, J. B. & Smith, J. E. (2007). *Ecol. Lett.* **10**, 1135–1142.
Eriksson, A. K., Hesterberg, D., Klysubun, W. & Gustafsson, J. P. (2016). *Sci. Total Environ.* **566–567**, 1410–1419.
Giguet-Covex, C., Poulenard, J., Chalmin, E., Arnaud, F., Rivard, C., Jenny, J. P. & Dorioz, J. M. (2013). *Geochim. Cosmochim. Acta*, **118**, 129–147.
Goebel, M., Adams, F., Boy, J., Guggenberger, G. & Mikutta, R. (2017). *J. Plant Nutr. Soil Sci.* **180**, 279–282.
Grand, S. & Lavkulich, L. M. (2015). *Plant Soil*, **390**, 77–93.
Harrison, A. F. (1987). *Soil Organic Phosphorus. A Review of World Literature*, p. 257. Wallingford: CAB International.
Hedley, M. J., Stewart, J. W. B. & Chauhan, B. S. (1982). *Soil Sci. Soc. Am. J.* **46**, 970–976.
Hesterberg, D., Zhou, W., Hutchison, K. J., Beauchemin, S. & Sayers, D. E. (1999). *J. Synchrotron Rad.* **6**, 636–638.
Hiemstra, T. & Van Riemsdijk, W. H. (1996). *J. Colloid Interface Sci.* **179**, 488–508.
Hunger, S., Sims, J. T. & Sparks, D. L. (2005). *J. Environ. Qual.* **34**, 382–389.
Johnson, B. B., Quill, E. & Angove, M. I. (2012). *J. Colloid Interface Sci.* **367**, 436–442.
Kaiser, K., Guggenberger, G. & Haumaier, L. (2003). *Biogeochemistry*, **66**, 287–310.
Kaiser, K., Guggenberger, G. & Zech, W. (2000). *Acta Hydrochim. Hydrob.* **28**, 411–419.
Khare, N., Hesterberg, D., Beauchemin, S. & Wang, S.-L. (2004). *Soil Sci. Soc. Am. J.* **68**, 460–469.
Khare, N., Hesterberg, D. & Martin, J. D. (2005). *Environ. Sci. Technol.* **39**, 2152–2160.
Klysubun, W., Sombunchoo, P., Deenan, W. & Kongmark, C. (2012). *J. Synchrotron Rad.* **19**, 930–936.
Kruse, J. & Leinweber, P. (2008). *J. Plant Nutr. Soil Sci.* **171**, 613–620.
Mehlich, A. (1984). *Commun. Soil Sci. Plant Anal.* **15**, 1409–1416.
Ognalaga, M., Frossard, E. & Thomas, F. (1994). *Soil Sci. Soc. Am. J.* **58**, 332–337.
Olsen, S. R., Cole, C. V., Watanabe, F. S. & Dean, L. A. (1954). *USDA Circular 939.* Washington DC: US Government Printing Office.
Persson, P., Nilsson, N. & Sjöberg, S. (1996). *J. Colloid Interface Sci.* **177**, 263–275.
Prietzel, J. (2017). *J. Plant Nutr. Soil Sci.* **180**, 14–17.
Prietzel, J., Dümig, A., Wu, Y., Zhou, J. & Klysubun, W. (2013). *Geochim. Cosmochim. Acta*, **108**, 154–171.
Prietzel, J., Harrington, G., Häusler, W., Heister, K., Werner, F. & Klysubun, W. (2016). *J. Synchrotron Rad.* **23**, 532–544.
Prietzel, J., Klysubun, W. & Werner, F. (2016). *J. Plant Nutr. Soil Sci.* **179**, 168–185.
Qualls, R. G., Haines, B. L. & Swank, W. T. (1991). *Ecology*, **72**, 254–266.
Qualls, R. G., Haines, B. L., Swank, W. T. & Tyler, S. W. (2000). *Soil Sci. Soc. Am. J.* **64**, 1068–1077.

Ravel, B. & Newville, M. (2005). *J. Synchrotron Rad.* **12**, 537–541.
Saunders, W. M. H. & Williams, E. G. (1955). *J. Soil Sci.* **6**, 254–267.
Schwertmann, U. & Cornell, R. M. (1991). *Iron Oxides in the Laboratory: Preparation and Characterization.* Weinheim: Verlag Chemie.
Shang, C., Stewart, J. W. B. & Huang, P. M. (1992). *Geoderma*, **53**, l–14.
Talkner, U., Jansen, M. & Beese, F. O. (2009). *Eur. J. Soil Sci.* **60**, 338–346.
Tejedor-Tejedor, M. I. & Anderson, M. A. (1986). *Langmuir*, **2**, 203–210.
Tiessen, H., Stewart, J. W. B. & Cole, C. V. (1984). *Soil Sci. Soc. Am. J.* **48**, 853–858.
Turner, B. L., Paphazy, M. J., Haygarth, P. M. & Mckelvie, I. D. (2002). *Philos. Trans. R. Soc. B: Biol. Sci.* **357**, 449–469.
Vincent, A. G., Schleucher, J., Gröbner, G., Vestergren, J., Persson, P., Jansson, M. & Giesler, R. (2012). *Biogeochemistry*, **108**, 485–499.
Walker, T. W. & Adams, A. F. R. (1958). *Soil Sci.* **85**, 307–318.
Werner, F., de la Haye, T. R., Spielvogel, S. & Prietzel, J. (2017). *Geoderma*, **302**, 52–65.
Werner, F. & Prietzel, J. (2015). *Environ. Sci. Technol.* **49**, 10521–10528.
Zederer, D. P. & Talkner, U. (2018). *Geoderma*, **325**, 162–171.